International Journal of Advances in Applied Sciences (IJAAS)
Vol. 1, No. 4, December 2012, pp. 159~170
ISSN: 2252-8814

A coupling method of Homotopy technique and Laplace transform for nonlinear fractional differential equations

Esmail Hesameddini, Mohsen Riahi, Habibolla Latifizadeh
Department of Mathematics, Faculty of Basic Sciences, Shiraz University of Technology, Shiraz, Iran

Article Info

Article history:

Received Aug 2, 2012
Revised Oct 29, 2012
Accepted Nov 27, 2012

Keyword:

Sharma-Tasso-Olver equation
Fisher equation
Laplace-Homotopy method
Analytical approximate solution.

ABSTRACT

In this work, the solutions of the fractional Sharma-Tasso-Olver (FSTO) and Fisher differential equations were investigated. The present study proposed a new novel and simple analytical method to obtain the solutions of FSTO and Fisher differential equations. Whereas, for nonlinear equations in general, no method is exists which yields to exact solution and therefore only approximate analytical solutions can be derived by using procedures such as linearization or perturbation. This method is combined form of the Laplace transformation and the Homotopy perturbation method. Advantage of the Laplace Homotopy Method (LHM), are simplicity of the computations, and non-requirement of linearization or smallness assumptions. For more illustration of the efficiency and reliability of LHM, some numerical results are depicted in different schemes and tables. Numerical results showed that the LHM was partly economical, efficient and precise to obtain the solution of nonlinear fractional differential equations.

Corresponding Author:

Habibolla Latifizadeh
Department of Mathematics, Faculty of Basic Sciences, Shiraz University of Technology, Shiraz, Iran
Email: H.Latifi.62.math@sutech.ac.ir – Habibolla Latifizadeh

1. INTRODUCTION

Fractional differential equations (FDEs) have long history. These equations have demonstrated a considerable interest both in mathematics and in applications in recent years. They have been used in modeling of many physical and chemical processes in engineering [1-3]. There are also applications in signal processing and sampling and hold algorithms, [4-6]. Fractional integral and derivatives can be of non-integer orders and even of complex order. The related fractional calculus facilitates the description of some problems which are not easy described by ordinary calculus due to modeling error [4-8]. There are different methods to solve the fractional differential equations. Some of the recent analytic methods for solving nonlinear problems are including the Adomian decomposition method (ADM) [9-11], Homotopy Perturbation Method (HPM) [12-14], Variational Iteration Method (VIM) [15,16] and Homotopy Analysis Method [17,18]. Partial differential equations of fractional order are often very complicated to be exactly solved and even if an exact solution is obtainable, the required calculations may be too complicated to be practical, or it might be difficult to interpret the outcome.

Finding accurate and efficient methods for solving FDEs become an important task. In this article, we use the HPM compound with the Laplace transform for solving the FDEs. The object of present paper is to extend the application of the LHM method to drive analytical approximate solutions for nonlinear fractional Sharma-Tasso-Olver and Fisher equations, so the model problems can be written as the following forms:

Case 1: The nonlinear fractional partial differential equation:

$$u_t^{\mu}+a\left(u^3\right)_x+\frac{3}{2}a\left(u^2\right)_{xx}+au_{xxx}=0, \tag{1}$$

is called Sharma-Tasso-Olver equation, where a is a real parameter, $u(x,t)$ is an unknown function depending on temporal variable t and spatial variable x . This equation contains both a linear dispersive term au_{xxx}, double nonlinear term $a\left(u^3\right)_x$ and $\frac{3}{2}a\left(u^2\right)_{xx}$. Many physicists and mathematicians have considered the Sharma-Tasso-Olver equation in recent years due to its appearance in scientific applications. To the explicit solution of integral models, various effective methods like inverse scattering transformation (IST) [19], Darboux transformation [20], Bäcklund transformation [21], solitary wave as well as periodic wave solutions [22], Kinks method, the tanh method, the extended tanh method [23], homogenous balance method [24], sine-cosine method [25], Jacobi elliptic method [26], F-expansion method [27] and etc. have been well developed.

Case 2: The nonlinear fractional Fisher differential equation is as follows:

$$u_t^{\mu} = u_{xx} - u^3 + (\varepsilon+1)u^2 - \varepsilon u,\ 0<\mu<1,\ 0<\varepsilon<1. \tag{2}$$

Fisher [28] proposed a reaction diffusion equation as a model to describe the process of spatial spreading when mutant individuals with higher adaptability appear in populations, namely:

$$u_t = u_{xx} + \alpha(1-u^{\beta})(u-\varepsilon),\ 0<\varepsilon<1, \tag{3}$$

where α, β and ε are parameters. This equation is well known in the field of population genetic. This equation is very important to fluid dynamic model and the study of this model has been considered by many authors both for conceptual understanding of physical flows and testing various numerical methods. Fisher equation has been found some applications in different fields as instances gas dynamics, number theory, heat conduction, elasticity etc. Ismail et al. [29]. Recently, Wazwaz and Gorguis [30] studied the Fisher equation, the general Fisher equation, and nonlinear diffusion equation of the Fisher type subject to initial conditions by using Adomian decomposition method. For more details about these investigations, many literatures are appeared [31-35].

2. BASIC DEFINITIONS AND NOTATIONS OF THE FRACTIONAL CALCULUS

In this section, some definitions and properties of the fractional calculus that will be used in this work are presented.

Definition 1. The Gamma function is intrinsically tied in fractional calculus. The simplest interpretation of the gamma function is simply the generalization of the fraction for all real numbers. The definition of the gamma function is given by:

$$\Gamma(\mu) = \int_0^{\infty} e^{-\xi}\xi^{\mu-1}d\xi,\ \text{for all } \mu\in\ . \tag{4}$$

Definition 2. The Riemann-Liouville fractional integral operator J^{μ} of order μ on the usual Lebesgue space $L_1[a,b]$ is given by:

$$\begin{aligned} J^{\mu}f(x) &= \frac{1}{\Gamma(\mu)}\int_0^x (x-\xi)^{\mu-1} f(\xi)d\xi, \\ J^0 f(x) &= f(x). \end{aligned} \tag{5}$$

It has the following properties:

$$\begin{aligned} &\text{(i) } J^{\mu} \text{ exists for any, } x\in[a,b],\ \mu>0, \\ &\text{(ii) } J^{\mu}J^{\beta}=J^{\beta}J^{\mu}=J^{\mu+\beta},\ \mu>0, \\ &\text{(iii) } J^{\mu}(x-\sigma)^{\gamma}=\frac{\Gamma(\gamma+1)}{\Gamma(\mu+\gamma+1)}(x-\sigma)^{\gamma+\mu},\ \mu\geq 0,\ \gamma>-1,\ \sigma\in\ . \end{aligned} \tag{6}$$

Definition 3. Let $f\in L_1[a,b]$, $m\in \square \bigcup\{0\}$, then the Caputo fractional derivative D_*^{μ} of $f(x)$ is defined as:

$$D_*^{\mu}=\begin{cases} J^{m-\mu}D_*^{m}f(x)=\dfrac{1}{\Gamma(m-\mu)}\displaystyle\int_0^x (x-\xi)^{m-\mu-1}\frac{d^m}{d\xi^m}f(\xi)d\xi, & \text{m-1<}\mu\text{<m},\\ \dfrac{d^m}{dx^m}f(x) & \mu=m. \end{cases} \tag{7}$$

It has the following basic properties:

$$\begin{aligned} &\text{(i) } D_*^{\frac{1}{2}}f(x)=J^{\frac{1}{2}}f'(x),\\ &\text{(ii) } D_*^{\mu}(x-\sigma)^{\gamma}=\frac{\Gamma(\gamma+1)}{\Gamma(\gamma-\mu+1)}(\text{x-}\sigma)^{\gamma-\mu},\ \mu\geq 0,\ \gamma>-1,\ \sigma\in\ ,\\ &\text{(iii) } D_*^{\mu}J^{\mu}f(x)=f(x),\ \mu\geq 0,\\ &\text{(iv) } J^{\mu}D_*^{\mu}f(x)=f(x)-\sum_{k=0}^{m-1}f^{k}(0^+)\frac{(x-\sigma)^k}{k!}. \end{aligned} \tag{8}$$

Definition 4. The Laplace transform of $f(x)$ is defined as follows:

$$F(s)=\ell\left[f(t);s\right]=\int_0^{\infty}e^{-st}f(t)dt. \tag{9}$$

Definition 5. The Laplace transform $\ell\left[f(t);s\right]$ of the Caputo fractional derivative is given by:

$$\ell\left[D_*^{\mu}f(t);s\right]=s^{\mu}F(s)-\sum_{k=0}^{m-1}s^{(\mu-k-1)}f^{(k)}(0^+),\ \text{F(s)=}\ell\left[f(t);s\right],\ m-1<\mu\leq m. \tag{10}$$

3. METHODOLOGY: ANALYSIS OF THE NOVEL PROPOSED METHOD

In order to demonstrate and clarify the basic ideas of the Laplace Homotopy Method (LHM), let us consider the following nonlinear differential equation:

$$L\left[u(x_1,\ldots,x_n)\right]+N\left[u(x_1,\ldots,x_n)\right]=\Re(x_1,\ldots,x_n), \tag{11}$$

where L is a linear operator, N is a nonlinear operator and $\Re(x_1,\ldots,x_n)$ is an inhomogeneous term. We can rewrite Eq. (11) down a correction functional as follows:

$$L_{x_i}\left[u(x_1,\ldots,x_n)\right]=\underbrace{\Re(x_1,\ldots,x_n)-\mathrm{M}\left[u(x_1,\ldots,x_n)\right]}_{RE\left[u(x_1,\ldots,x_n)\right]}, \tag{12}$$

where M is a nonlinear operator that has been embraced the nonlinear source and the rest of the other linear operator of Eq. (11). In addition we have $L_{x_i}\left[u(x_1,\ldots,x_n)\right]=\sum_k\left(L_{x_i}^k\left[u(x_1,\ldots,x_n)\right]\right)$. Therefore by taking Laplace transform to both sides of Eq. (12) in the usual way and using the initial conditions, one obtain the result as follows:

$$p(s)U(x_1,\ldots,x_{i-1},s,x_{i+1},\ldots,x_n)=\sum_{\eta=0}^{m-1}\left(s^{m-\eta-1}\frac{\partial^{\eta}u(x_1,\ldots,x_{i-1},0,x_{i+1},\ldots,x_n)}{\partial(x_i)^{\eta}}\right)+\ell\left[RE\left[u(x_1,\ldots,x_n)\right];s\right] \tag{13}$$

where $p(s)$ is a polynomial with the degree of the highest partial derivative in Eq. (12), and also $\ell\left[RE\left[u(x_1,\ldots,x_n)\right];s\right]$ is Laplace transform of $RE\left[u(x_1,\ldots,x_n)\right]$.

Supposing the initial conditions, we set:

$$\frac{\partial^{\delta}}{\partial(x_i)^{\delta}}u(x_1,\ldots,x_{i-1},0,x_{i+1},\ldots,x_n)=d_{\delta}(x_1,\ldots,x_{i-1},0,x_{i+1},\ldots,x_n),\ \delta=1,2,\ldots,m-1. \tag{14}$$

By using the convolution theorem and applying the inverse Laplace transform to both sides of Eq. (13), result in:

$$u(x,\dots,x_{i-1},x_i,x_{i+1},\dots,x_n)=\ell^{-1}\left[\sum_{\eta=0}^{m-1}\left(\frac{s^{m-\eta-1}}{p(s)}d_\eta(x_1,\dots,x_{i-1},0,x_{i+1},\dots,x_n)\right);s\right]+ \\ +\int_0^{x_i}RE\left[u(x_1,\dots,x_{i-1},x_\tau,x_{i+1},\dots,x_n)\right]f(x_i-\tau)d\tau, \tag{15}$$

where $F(s)=\dfrac{1}{p(s)}$, $\ell[f(x_i);s]=F(s)$, and also for simplicity is supposed that:

$$A=\ell^{-1}\left[\sum_{\eta=0}^{m-1}\left(\frac{s^{m-\eta-1}}{p(s)}d_\eta(x_1,\dots,x_{i-1},0,x_{i+1},\dots,x_n)\right);s\right], \tag{16}$$

$$\hbar=\int_0^{x_i}RE\left[u(x_1,\dots,x_{i-1},x_\tau,x_{i+1},\dots,x_n)\right]f(x_i-\tau)d\tau. \tag{17}$$

Now a new operator entitled the Homotopy operator [12-14] $\mathrm{H}\left(u(x_1,\dots,x_n),p\right):\Omega\times[0,1]\to\mathbb{R}$ can be defined in the following way which is the principle idea of this technique:

$$\mathrm{H}\left(u(x_1,\dots,x_n),p\right)=u(x_1,\dots,x_n)-\hbar(u(x_1,\dots,x_n))-pA(x_1,\dots,x_n)=0, \tag{18}$$

where $p\in[0,1]$ is a Homotopy parameter and u_0 is an initial approximation which satisfies the boundary conditions. Obviously for $p=0$, $p=1$, Eq. (18) reduces to the following equations respectively:

$$\mathrm{H}\left(u(x_1,\dots,x_n),0\right)=u(x_1,\dots,x_n)-\hbar(u(x_1,\dots,x_n)), \tag{19}$$

$$\mathrm{H}\left(u(x_1,\dots,x_n),1\right)=u(x_1,\dots,x_n)-\hbar(u(x_1,\dots,x_n))-A(x_1,\dots,x_n)=0. \tag{20}$$

So while changing the values of p from zero to unity, $u(x_1,\dots,x_n)$ will be changed from u_0 to u. In topology, this is called deformation, while $u-\hbar(u)$ and $u-\hbar(u)-A$ are called Homotopic. Using the Homotopy parameter p, the following power series can be presented for u:

$$u(x_1,\dots,x_n)=\sum_{\gamma=0}^{\infty}p^\gamma u_\gamma(x_1,\dots,x_n). \tag{21}$$

Assuming that:

$$RE\left[u(x_1,\dots,x_n)\right]=\sum_{\gamma=0}^{\infty}p^\gamma H_\gamma(u_1,\dots,u_\gamma), \tag{22}$$

homotopy equation will be written as follows:

$$\sum_{\gamma=0}^{\infty}p^\gamma u_\gamma(x_1,\dots,x_n)=A+p\left[\int_0^{x_i}\sum_{\gamma=0}^{\infty}p^\gamma H_\gamma(u_1,\dots,u_\gamma)f(x_i-\tau)d\tau\right]. \tag{23}$$

This has been raised by coupling of the Laplace transform and the Homotopy technique. Comparing the coefficients of the like powers of p, the following approximations are obtained:

$$\begin{aligned} &p^0:\ u_0=A,\\ &p^1:\ u_1=\int_0^{x_i}H_0(u_0)f(x_i-\tau)d\tau,\\ &p^2:\ u_2=\int_0^{x_i}H_0(u_0,u_1)f(x_i-\tau)d\tau,\\ &\quad\vdots\\ &p^\gamma:\ u_\gamma=\int_0^{x_i}H_0(u_0,u_1,\dots,u_\gamma)f(x_i-\tau)d\tau. \end{aligned} \tag{24}$$

If the series (21) is convergent then, by taking $p=1$, one obtain the approximate solution of equation (11) as follows:

$$u=\lim_{p\to1}\sum_{\gamma=0}^{\infty}p^\gamma u_\gamma=u_0+u_1+u_2+u_3+\cdots. \tag{25}$$

4. APPLICATIONS OF THE LAPLACE HOMOTOPY METHOD (LHM)

In order to illuminate the procedure of Laplace Homotopy Method (LHM), the solution of the fractional Sharma-Tasso-Olver and Fisher differential equations will be studied.

Example 1: We consider the fractional Sharma-Tasso-Olver equation by utilization of LHM which was explained in section 3. This equation is as follows:

$$u_t^{\mu} + aD_x u^3 + \frac{3}{2}aD_{xx}u^2 + aD_{xxx}u = 0,\ 0 < \mu \le 1, \tag{26}$$

with the initial condition:

$$u(x,0) = 2k\,\frac{e^{kx+w}}{e^{kx+w}+r} - k. \tag{27}$$

In this case μ is a constant and lies in the interval $(0,1]$, t and x are time and spatial coordinates respectively, a is a real parameter and k, w and r are free parameters.

The exact solution of (26) for $\mu = 1$ is [21]:

$$u(x,t) = 2k\,\frac{e^{kx-ak^3t+w}}{e^{kx-ak^3t+w}+r} - k. \tag{28}$$

Applying the LHM to Eq. (26), the result is as follows:

$$U(x,s) = \frac{s^{\mu-1}}{s^{\mu}}u(x,0) - \frac{1}{s^{\mu}}\ell\left[aD_x u^3 + \frac{3}{2}aD_{xx}u^2 + a\,D_{xxx}u; s\right]. \tag{29}$$

Benefiting the inverse Laplace transform to both sides of Eq. (29), and subsequently constructing the Homotopy function, one obtain:

$$u(x,t) = 2k\,\frac{e^{kx+w}}{e^{kx+w}+r} - k - p\int_0^t RE\left[u(x,\tau)\right]\frac{(t-\tau)^{\mu-1}}{\Gamma(\mu)}d\tau, \tag{30}$$

where:

$$RE\left[u(x,\tau)\right] = -\left(aD_x u^3(x,\tau) + \frac{3}{2}aD_{xx}u^2(x,\tau) + a\,D_{xxx}u(x,\tau)\right). \tag{31}$$

Assuming the solution of Eq. (26) as a power series in the form of:

$$u(x,t) = u_0 + pu_1 + p^2u_2 + p^3u_3 + \cdots, \tag{32}$$

and substituting in (31), results in:

$$RE\left[u(x,\tau)\right] = -p^0H_0(u_0(x,\tau)) - p^1H_1(u_0(x,\tau),u_1(x,\tau)) - p^2H_2(u_0(x,\tau),u_1(x,\tau),u_2(x,\tau)) - \cdots, \tag{33}$$

where:

$$\begin{aligned}
H_0(u_0) &= -3au_0^2D_xu_0 - \frac{3}{2}a\left\{\left(2D_xu_0\right)^2 + 2u_0D_{xx}u_0\right\} - aD_{xxx}u_0,\\
H_1(u_0,u_1) &= -a\left\{3u_0^2D_xu_1 + 3u_1D_{xx}u_0 + 6D_xu_0D_xu_1 + 6u_0u_1D_xu_0 + 3u_0D_{xx}u_1 + D_{xxx}u_1\right\},\\
H_2(u_0,u_1,u_2) &= -a\left\{3u_0^2D_xu_1 + 6u_0u_1D_xu_1 + 3\left(2u_0u_2 + u_1^2\right)D_xu_0 + 3u_0D_{xx}u_2 + 3u_1D_{xx}u_1 + 3u_2D_{xx}u_0 + \right.\\
&\quad \left. + 6D_xu_0D_xu_2 + D_{xxx}u_2,\right.\\
&\ \ \vdots,
\end{aligned} \tag{35}$$

and so on. By considering $u_0(x,t) = 2k\,\frac{e^{kx+w}}{e^{kx+w}+r} - k$, and substituting (35) in (33) also equating the coefficients of the like powers of p, one gets the following set of equations:

$$\begin{aligned}
u_1(x,t) &= \int_0^t H_0(u_0)\frac{(t-\tau)^{\mu-1}}{\Gamma(\mu)}d\tau,\\
u_2(x,t) &= \int_0^t H_1(u_0,u_1)\frac{(t-\tau)^{\mu-1}}{\Gamma(\mu)}d\tau,\\
&\ \ \vdots,
\end{aligned} \tag{36}$$

after some simplification and substitution, the following set of equations are resulted:

$$
\begin{aligned}
u_0(x,t) &= 2k\,\frac{e^{kx+w}}{e^{kx+w}+r}-k,\\
u_1(x,t) &= -2ak^4\,\frac{re^{kx+w}}{(e^{kx+w}+r)^2}\int_0^t\frac{(t-\tau)^{\mu-1}}{\Gamma(\mu)}d\tau=-2ak^4\,\frac{re^{kx+w}}{(e^{kx+w}+r)^2}J_t^{\mu}(1)=-2ak^4\,\frac{re^{kx+w}}{(e^{kx+w}+r)^2\Gamma(\mu+1)}t^{\mu},\\
u_2(x,t) &= -2a^2k^7\,\frac{re^{kx+w}(e^{kx+w}-r)}{(e^{kx+w}+r)^3\Gamma(\mu+1)}\int_0^t\frac{(t-\tau)^{\mu-1}\tau^{\mu}}{\Gamma(\mu)}d\tau=-2a^2k^7\,\frac{re^{kx+w}(e^{kx+w}-r)}{(e^{kx+w}+r)^3\Gamma(\mu+1)}J_t^{\mu}(t^{\mu})=\\
&= -2a^2k^7\,\frac{re^{kx+w}(e^{kx+w}-r)}{(e^{kx+w}+r)^3\Gamma(2\mu+1)}t^{2\mu},\qquad (37)\\
u_3(x,t) &= -2a^3k^{10}\,\frac{re^{kx+w}(e^{2(kx+w)}-4re^{kx+w}+r^2)}{(e^{kx+w}+r)^4\Gamma(2\mu+1)}\int_0^t\frac{(t-\tau)^{\mu-1}\tau^{2\mu}}{\Gamma(\mu)}d\tau=\\
&= -2a^3k^{10}\,\frac{re^{kx+w}(e^{2(kx+w)}-4re^{kx+w}+r^2)}{(e^{kx+w}+r)^4\Gamma(2\mu+1)}J_t^{\mu}(t^{2\mu})=\\
&= -2a^3k^{10}\,\frac{re^{kx+w}(e^{2(kx+w)}-4re^{kx+w}+r^2)}{(e^{kx+w}+r)^4\Gamma(3\mu+1)}t^{3\mu},\\
&\ \vdots,
\end{aligned}
$$

where k, w and r are constants.
Therefore, the solution in a series form is given by:

$$u(x,t)=u_0(x,t)+u_1(x,t)+u_2(x,t)+u_3(x,t)+\cdots. \qquad (38)$$

I. Numerical Results for space-and time fractional Sharma-Tasso-Olver equation

In this subsection, the space and time fractional Sharma-Tasso-Olver equation is considered for numerical comparisons. In order to numerically verify whether the proposed methodology leads to higher accuracy, the approximate solution was evaluated by using n-term approximation in (38). In Fig. 1 $u(x,t)=\sum_{\gamma=0}^{5}u_{\gamma}$ and the exact solution have been depicted for $\mu=1$, $k=1$, $t=0.1$, $a=1$, r=1, $w=\frac{1}{2}$, Moreover, Fig. 2 illustrates the approximate solutions of the equation which was obtained for different values of μ and $k=1$, $t=0.1$, $a=1$, r=1, $w=\frac{1}{2}$, by using the LHM. In Fig. 3(a) -(c), the behavior of $u(x,t)$ is given. Numerical results obtained by these approximations are summarized in Tables 1 and, 2. It is clear that the approximate solutions converge to the exact solution. In addition, these tables demonstrate the comparison between the exact values of $u(x,t)$ and its approximate values by LHM when $t=0.01$, $\mu=1$. Accordingly in this table, a very interesting agreement between the results is observed, which confirms the excellent validity of the LHM. In figures 4(a)- (c) and 5(a) -(c) the error function of Eq. (26) which is resulted by LHM are depicted.

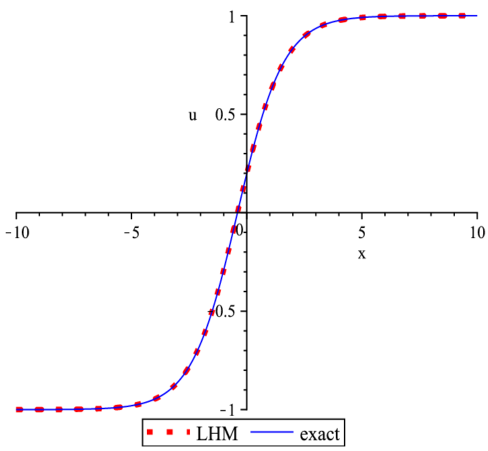

Fig. 1 Comparison between LHM solution and the exact solution for $\mu=1$ and $t=0.1$

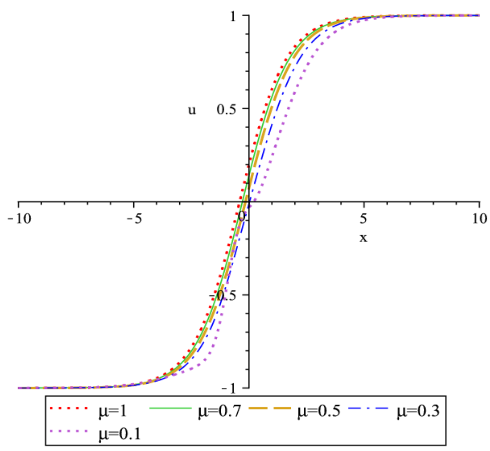

Fig. 2 Plot solutions of (4.1) when $\mu=1$, $\mu=0.7$, $\mu=0.5$, $\mu=0.3$, $\mu=0.1$ and $t=0.1$

Table 1. Comparison between the exact values of $u(x,t)$ and its approximate values obtained by LHM

t	$t = 0.01$		Absolute error
	Exact value	Approximate value	
0	0.240212864686635	0.24021286468618	4.55×10^{-13}
1	0.632156545160594	0.63215654516099	3.96×10^{-13}
2	0.846875605296253	0.84687560529638	1.27×10^{-13}
3	0.940803791641747	0.94080379164172	2.7×10^{-14}
4	0.977807724005105	0.97780772400508	2.5×10^{-14}
5	0.991778249755353	0.99177824975534	1.3×10^{-14}
6	0.996967506973151	0.99696750697314	1.1×10^{-14}
7	0.998883337894465	0.99888333789447	5.1×10^{-15}
8	0.999589057933814	0.99958905793381	4.1×10^{-15}
9	0.999828803224529	0.99984880322453	1.1×10^{-15}
10	0.999944375156570	0.99994437515657	0.0

Table 2. Comparison between the exact values of $u(x,t)$ and its approximate values obtained by LHM

(x,t)	Exact value	Approximate value	Absolute error
$(\mathbf{5}, -\mathbf{0.5})$	0.99505475368673	0.995051163053026	3.591×10^{-6}
$(\mathbf{4}, -\mathbf{0.4})$	0.98521691731144	0.985414412948829	2.5×10^{-6}
$(\mathbf{3}, -\mathbf{0.3})$	0.95623745812774	0.956236877347742	5.81×10^{-7}
$(\mathbf{2}, -\mathbf{0.2})$	0.87405328788601	0.874053657051266	3.69×10^{-7}
$(\mathbf{1}, -\mathbf{0.1})$	0.66403677026785	0.664036810289600	2.002×10^{-8}
$(\mathbf{0}, \mathbf{0})$	0.24491866240371	0.244918662403709	0.
$(\mathbf{1}, \mathbf{0.1})$	0.60436777711716	0.604367737127432	3.999×10^{-8}
$(\mathbf{2}, \mathbf{0.2})$	0.81775407797029	0.817753678438746	3.995×10^{-7}
$(\mathbf{3}, \mathbf{0.3})$	0.92166855440647	0.921669089642980	5.352×10^{-7}
$(\mathbf{4}, \mathbf{0.4})$	0.96739500125712	0.967397599250401	2.598×10^{-6}
$(\mathbf{5}, \mathbf{0.5})$	0.98661429815143	0.986618155057450	3.857×10^{-6}

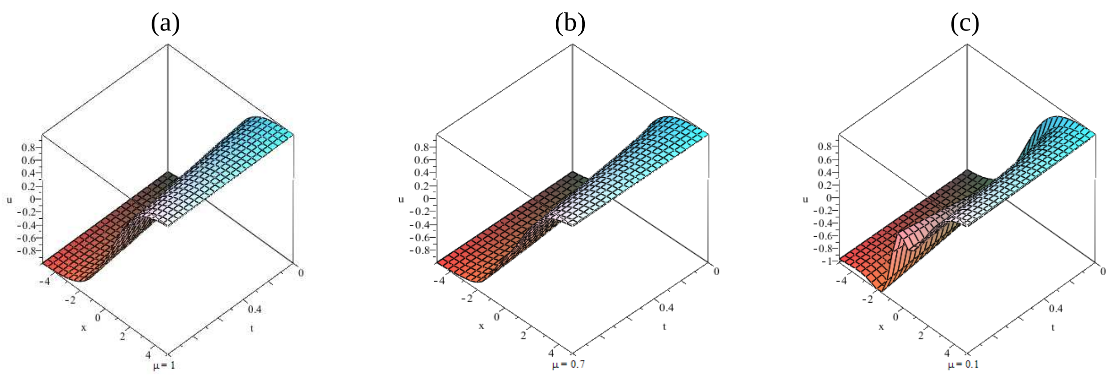

Fig. 3 Graphs of $u(x,t)$, where (a) $\mu = 1$, (b) $\mu = 0.7$ and (c) $\mu = 0.1$

It is admirable and easy to verify the accuracy of the results for different values of μ graphically. Additionally, these figures demonstrate that the errors of LHM increased in the neighborhood of critical point $x = 0$ and overall indicate that the differences among the LHM and the real solution are negligible. Meanwhile, it is worth mentioning that a higher accuracy can be obtained by evaluating some more terms of the series solution.

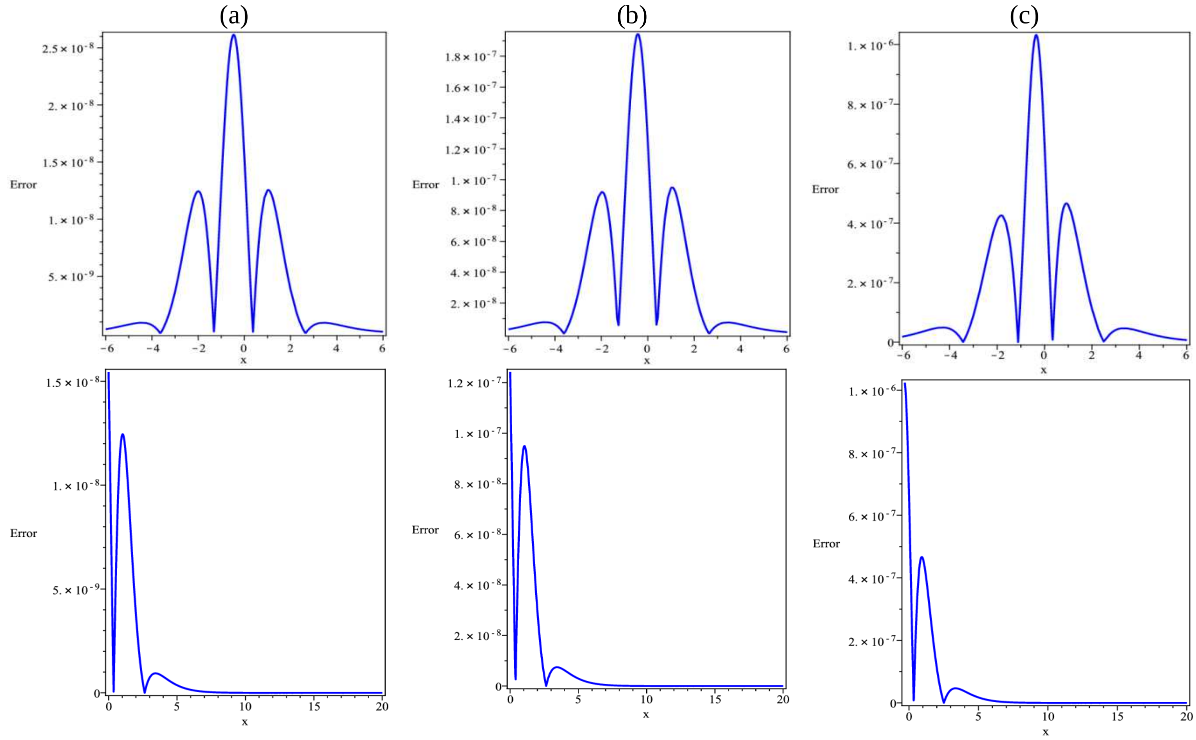

Fig. 4 Graphs of the absolute error functions for different values of μ, $k=1$, r=1, $w=\frac{1}{2}$, $t=\frac{1}{2}$ and $a=0.1$, when (a) $\mu=1$, (b) $\mu=\frac{3}{4}$, (c) $\mu=\frac{1}{2}$

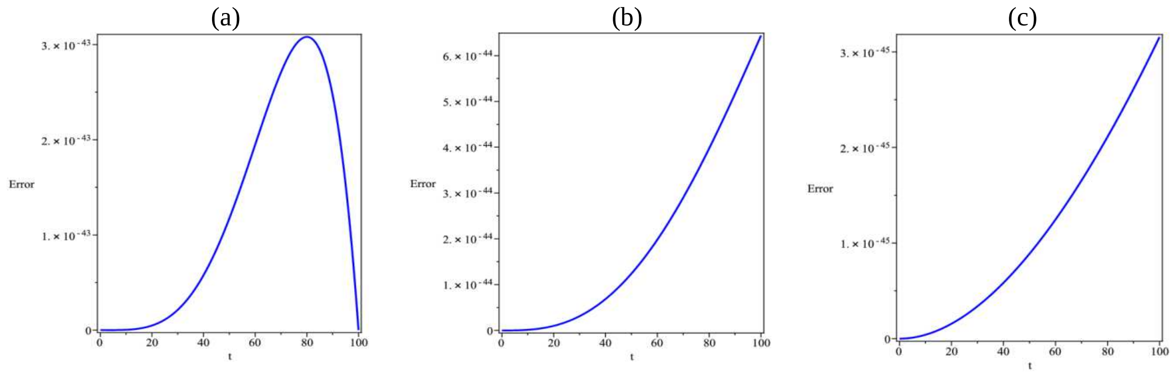

Fig. 5 Graphs of the absolute error functions for different values of μ, $x=100$, $k=1$, r=1, $w=\frac{1}{2}$, and $a=0.1$, when (a) $\mu=1$, (b) $\mu=\frac{3}{4}$, (c) $\mu=\frac{1}{2}$

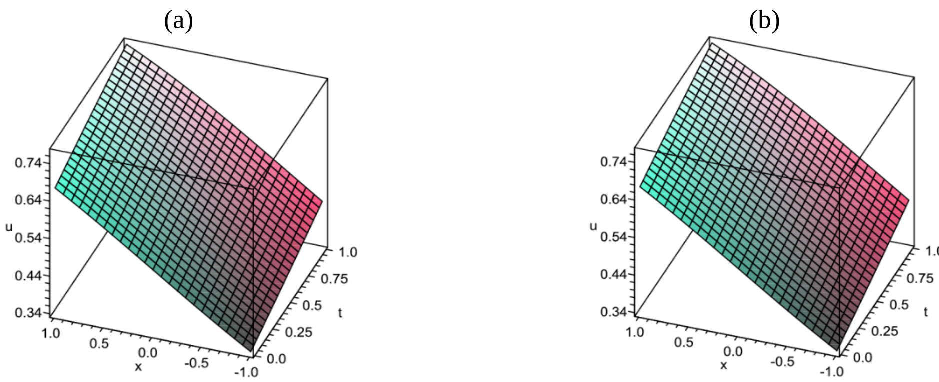

Fig. 6. Comparison between the results of the LHM and the exact solution for the fractional Fisher equation when $\mu=1$, $\varepsilon=0.01$. (a) approximate solution, (b) exact solution.

Table 3: Comparison between the exact values of $u(x,t)$ and its approximate values obtained by LHM when $\varepsilon = 0.5$, $\mu = 1$.

(x,t)	Exact	Approximate	Absolute error
(0,0.0)	0.750000000000	0.750000000000	0
(2,0.2)	0.843066997899	0.843066997434	4.65×10^{-10}
(4,0.4)	0.913478570290	0.913478607880	3.76×10^{-8}
(6,0.6)	0.956320652061	0.956320819437	1.67×10^{-7}
(8,0.8)	0.979025112311	0.979025218777	1.06×10^{-7}
(10, 1)	0.990181755428	0.991815142291	2.41×10^{-7}

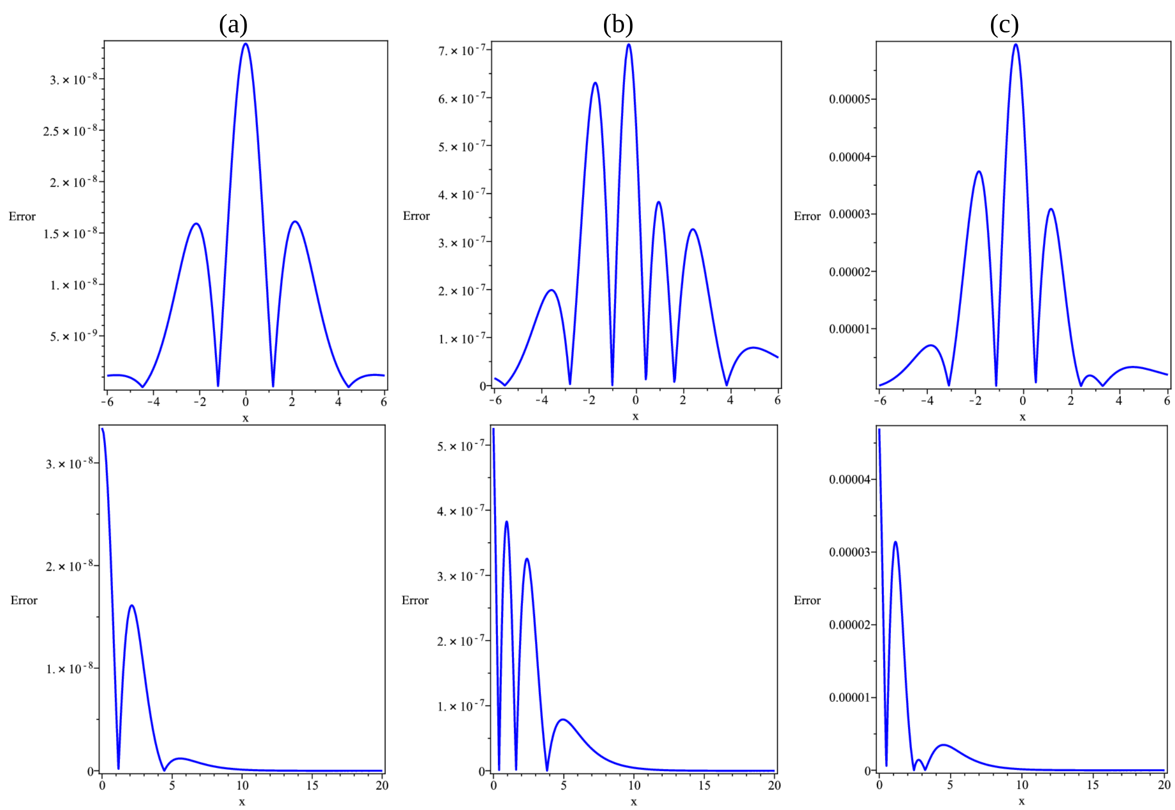

Fig. 7: Graphs of the absolute error functions for different values of μ, $\varepsilon = 0.01$ and $t = 0.1$, when (a) $\mu = 1$, (b) $\mu = \frac{3}{4}$, (c) $\mu = \frac{1}{2}$

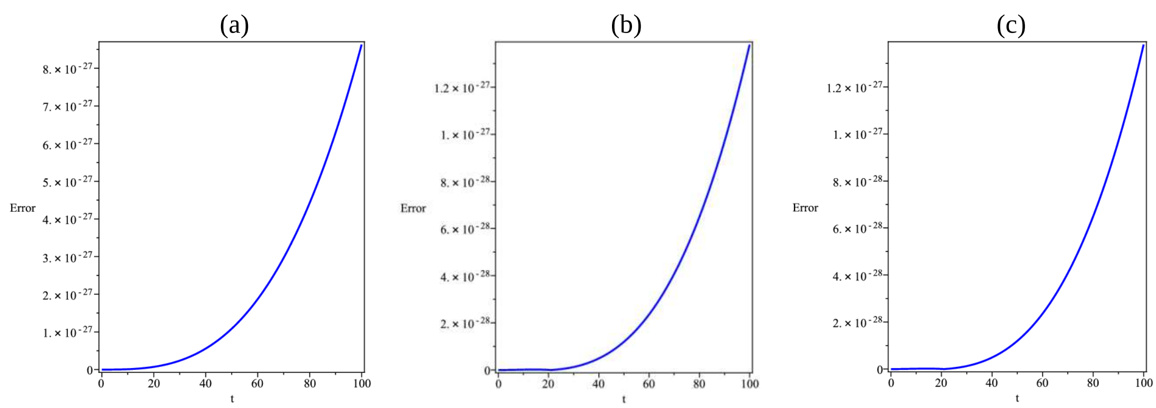

Fig. 8: Graphs of the absolute error functions for different values of μ, $x = 100$ and $\varepsilon = 0.01$, when (a) $\mu = 1$, (b) $\mu = \frac{3}{4}$, (c) $\mu = \frac{1}{2}$

Example 2: (Fisher equation) Consider the nonlinear time fractional diffusion equation of the form:

$$D_t^{\mu} u = D_{xx} u - u^3 + (\varepsilon+1)u^2 - \varepsilon u, \; 0<\mu<1, \; 0<\varepsilon<1, \tag{39}$$

subjected to the initial condition:

$$u(x,0) = \frac{\varepsilon + e^{-\left(\frac{1}{\sqrt{2}}(\varepsilon-1)x\right)}}{1+e^{-\left(\frac{1}{\sqrt{2}}(\varepsilon-1)x\right)}}. \tag{40}$$

The exact solution of (39) and it's traveling wave solution of the form:

$$u(x,t) = \frac{1}{2}(\varepsilon+1) + \frac{1}{2}(1-\varepsilon)\tanh\left[\frac{\sqrt{2}}{4}(1-\varepsilon)x + \frac{1}{4}\left(1-\varepsilon^2\right)t\right], \tag{41}$$

or equivalently:

$$u(x,t) = \frac{1}{2}(\varepsilon+1) + \frac{1}{2}(1-\varepsilon)\frac{e^{-\frac{1}{4}(1-\varepsilon)\left(\sqrt{2}+(1+\varepsilon)t\right)} + e^{\frac{1}{4}(1-\varepsilon)\left(\sqrt{2}+(1+\varepsilon)t\right)}}{e^{-\frac{1}{4}(1-\varepsilon)\left(\sqrt{2}+(1+\varepsilon)t\right)} - e^{\frac{1}{4}(1-\varepsilon)\left(\sqrt{2}+(1+\varepsilon)t\right)}}, \tag{42}$$

is given in [36].
Applying the Laplace transform to both sides of Eq. (39), we have:

$$U(x,s) = \frac{s^{\mu-1}}{s^{\mu}}u(x,0) + \frac{1}{s^{\mu}}\ell\left[D_{xx}u - u^3 + (\varepsilon+1)u^2 - \varepsilon u; s\right]. \tag{43}$$

According to the LHM:

$$u(x,t) = \frac{\varepsilon + e^{-\left(\frac{1}{\sqrt{2}}(\varepsilon-1)x\right)}}{1+e^{-\left(\frac{1}{\sqrt{2}}(\varepsilon-1)x\right)}} + p\int_0^t RE\left[u(x,\tau)\right]\frac{(t-\tau)^{\mu-1}}{\Gamma(\mu)}d\tau, \tag{44}$$

where:

$$RE\left[u(x,\tau)\right] = D_{xx}u - u^3 + (\varepsilon+1)u^2 - \varepsilon u. \tag{45}$$

Assuming the solution of Eq. (39) as a power series in the form of:

$$u(x,t) = u_0 + pu_1 + p^2u_2 + p^3u_3 + \cdots, \tag{46}$$

and substituting in (45), one obtain:

$$RE\left[u(x,\tau)\right] = -p^0H_0(u_0(x,\tau)) - p^1H_1(u_0(x,\tau),u_1(x,\tau)) - p^2H_2(u_0(x,\tau),u_1(x,\tau),u_2(x,\tau)) - \cdots, \tag{47}$$

where:

$$\begin{aligned}
&H_0(u_0) = D_{xx}u_0 - u_0^3 + (\varepsilon+1)u_0^2 - \varepsilon u_0,\\
&H_1(u_0,u_1) = D_{xx}u_1 - 3u_0^2u_1 + 2(\varepsilon+1)u_0u_1,\\
&H_2(u_0,u_1,u_2) = D_{xx}u_2 - 3u_0^2u_2 + 2(\varepsilon+1)u_0u_2 + (\varepsilon+1)u_1^2 - \varepsilon u_2,\\
&H_3(u_0,u_1,u_2) = D_{xx}u_3 - 3u_0^2u_3 + 2(\varepsilon+1)u_1u_2 + 2(\varepsilon+1)u_0u_3 - 6u_0u_1u_2 - u_1^3 - \varepsilon u_3,\\
&\quad\vdots
\end{aligned} \tag{48}$$

Considering $u_0(x,t) = \dfrac{\varepsilon + e^{-\left(\frac{1}{\sqrt{2}}(\varepsilon-1)x\right)}}{1+e^{-\left(\frac{1}{\sqrt{2}}(\varepsilon-1)x\right)}}$ and substituting in (48), also equating the coefficients of the like powers of p, one gets the following set of equations:

$$\begin{aligned}
&u_1(x,t) = \int_0^t H_0(u_0)\frac{(t-\tau)^{\mu-1}}{\Gamma(\mu)}d\tau,\\
&u_2(x,t) = \int_0^t H_1(u_0,u_1)\frac{(t-\tau)^{\mu-1}}{\Gamma(\mu)}d\tau,\\
&\quad\vdots
\end{aligned} \tag{49}$$

Assuming $e^{-\left(\frac{1}{\sqrt{2}}(\varepsilon-1)x\right)} = A$, after some simplification and substitution, the following set of equations are resulted:

$$u_0(x,t) = \frac{\varepsilon + A}{1+A},$$

$$u_1(x,t)=\frac{1}{2}\frac{A(\varepsilon+1)(\varepsilon-1)^2}{(A+1)^2\Gamma(\mu+1)}t^{\mu}, \tag{50}$$
$$u_2(x,t)=\frac{1}{4}\frac{A(A-1)(\varepsilon+1)^2(\varepsilon-1)^3}{(A+1)^3\Gamma(2\mu+1)}t^{2\mu},$$
$$\vdots,$$

and so on. In the same manner the rest of the other components can be obtained by using the Maple package.

II. Numerical Results for space-and time fractional Fisher equation

In this subsection we present the results of LHM to show the efficiency of this method. Table 3 shows the approximate solution by 5-terms, exact solution and absolutely error obtained by LHM, when $\varepsilon=0.5$, $\mu=1$. It is evident that the efficiency of this approach can be dramatically enhanced by computing further terms of $u(x,t)$. In Fig. 6(a) we plot the 5-term LHM approximate solutions for $\varepsilon=0.01$ and $\mu=1$. In 1(b) the plot of the exact solution when $\mu=1$ and $\varepsilon=0.01$ is depicted. In figures 7(a)- (c) and 8(a) -(c) the error function of Eq. (39) which is resulted by LHM are illustrated. It is admirable and easy to verify the accuracy of the results for different values of μ graphically. Additionally, these figures demonstrate that the errors of LHM increased in the neighborhood of critical point $x=0$ and overall indicate that the differences among the LHM and the real solution are negligible. Also in table 3, a very interesting agreement between the results is observed, which confirms the excellent validity of the LHM. Meanwhile it is worth mentioning that a higher accuracy can be obtained by evaluating some more terms of the series solution.

5. CONCLUSION

In this paper, a novel and interesting but rigorous Laplace Homotopy Method (LHM) has been utilized to derive the approximate analytical solutions for nonlinear fractional Sharma-Tasso-Olver and fractional Fisher equations. To demonstrate the validity of the proposed method, numerical results have been obtained which shows that the LHM strength lays in its ease of use and the possibility of using it as a tool to acquire approximate solutions of nonlinear fractional differential equation with excellent accuracy by applying a few iterations.

REFERENCES

[1] O. Heaviside, Electromagnetic Theory, Chelsea, New York, 1971.
[2] N. Laskin, Fractional market dynamics, physica A 287 (2000) 482-492.
[3] D. Kusnezov, A. Bulgac, G.D. Dang, Quantum Levy processes and fractional kinetics, Phys. Rev. Lett. 82 (1999) 1136-1139.
[4] Y. Luchko and R. Gorenflo, “An operational method for solving fractional differential equations with the Caputo derivatives”, Acta Mathematica Vietnamica, Vol. 24, No. 2, pp. 207-233, 1999.
[5] Yu. F. Luchko and H.M. Srivastava, “Differential equations of fractional order by using operational calculus”, Computers and Mathematics with Applications, Vol. 29, No. 8 , pp. 73-85, 1995.
[6] S. Das, Functional Fractional calculus for System Identification and Controls, Springer–Verlag, Berlin, 2008.
[7] L.A. Zadeh and C. A. Desoer, Linear System Theory, McGraw- Hill, New York, 1963.
[8] K. Oldham and J. Spanier, The fractional Calculus. Theory and Applications of Differentiation and Integration to Arbitrary Order, Dover Publications INC, Mineola, New York, 1974.
[9] G. Adomian, Areview of the decomposition method and some recent results for nonlinear equation, Math.Compute. Model. 13 (7) (1992) 17.
[10] J.-S. Duan, R. Rach, A new modification of the adomian decomposition method for solving boundary value problems for higher order nonlinear differential equations, Appl. Math. Comput. 218 (2011) 4090-4118.
[11] M. Kumar, N. Singh, Modified Adomian Decomposition Method and computer implementation for solving singular boundary value problems arising in various physical problems, Computers and Chemical Engineering 34 (2010) 1750-1760.
[12] J.H. He, homotipy perturbation technique, Comput. Methods Appl. Mech. Engrg. 178 (1999) 257-262.
[13] J.H. He, A coupling method of homotopy tecknique and perturbation tecknique for nonlinear problems, Int. J. Nonlinear Mech. 35 (2000) 37-43.
[14] Odibat Z, Momani S. Modified homotopy perturbation method: application to quadratic Riccati differential equation of fractional order. Chaos Solitons Fractals 2008;36:167–74.
[15] Odibat Z, Momani S. Application of variational iteration method to nonlinear differential equation of fractional order. Int J Nonlinear Sci Numer Simul 2006;1(7):271–9.
[16] Momani S, Odibat Z. Numerical comparison of methods for solving linear differential equations of fractional order. Chaos Solitons Fractals 2007;31:1248–55.

[17] S. J. Liao, on the proposed homotopy analysis technique for nonlinear problems and its applications, Ph.D. Dissertation. Shanghai Jiao Tong University, Shanghai, 1992.
[18] S. J. Liao, On the homotopy analysis method for nonlinear problems. Appl Math Comput 2004; 499-513.
[19] C.S. Gardner, J.M. Greene, M.D. Kruskal, R.M. Miura, Phys. Rev. Lett. 19 (1967) 1095.
[20] V.B. Matveev, M.A. Salle, Darboux Transformations and Solitons, Springer, Berlin, Heidelberg, 1991.
[21] Y. Shang, Y. Huang, W. Yuan, Bäcklund transformations and abundant exact explicit solutions of the Sharma-Tasso-Olver equation, Comput. Math. Appl. 217 (2011) 7172-7183.
[22] Y. Shang, J. Qin, Y. Huang, W. Yuan, Abundant exact and explicit solitary Wave and periodic Wave solutions to the Sharma-Tasso-Olver equation, Comput. Math. Appl. 202 (2008) 532-538.
[23] A.M. Wazwaz, New solitons and kinks solutions to the Sharma-Tasso-Olver equation, Comput. Math. Appl. 188 (2007) 1205-1213.
[24] M.L. Wang, Exact solutions for a compound Kdv-Burger equation, Phys. Lett. A, 213 (5-6) (1996) 87-279.
[25] A.M. Wazwaz, S sine-cosine method for handling nonlinear Wave equations, Comput. Math. Model 40 (5-6) (2004) 499-508.
[26] X.Q. Zhao, H.Y. Zhi, H.Q. Zhang, Improved Jacobi-function method with symbolic computation to construct new double-periodic solutions for the generalized Ito system, Chaos Solitons Fractals 28 (1) (2006) 26-112.
[27] M.A. Abdou, extended F-expansion method and its application for a class of nonlinear evolution equations, Chaos Solitons Fractals 31 (1) (2007) 95-104.
[28] R.A. Fisher, The wave of advance of advantageous genes, Ann. of Eugenics 7 (1937) 255–369.
[29] H.N.A. Ismail, K. Raslan, A.A.A. Rabboh, Adomian decomposition method for Burgers' Huxley and Burgers–Fisher equations, Appl. Math. Comput. 159 (2004) 291–301.
[30] A.M. Wazwaz, A. Gorguis, An analytical study of Fisher's equation by using Adomian decomposition method, Applied Mathematics and Computation 154 (2004) 609-20.
[31] J. Sheratt, On the transition from initial data traveling waves in the Fisher-KPP equation, Dynamics and Stability of Systems 13 (2) (1998) 167-174.
[32] P. Brazhnik, J. Tyson, On traveling wave solutions of Fisher's equation in two spatial dimensions, SIAM Journal on Applied Mathematics 60 (2) (1999) 371-391.
[33] W. Malfliet, Solitary wave solutions of nonlinear wave equations, American Journal of Physics 60 (7) (1992) 650654.
[34] M. Alowitz, A. Zepetella, Explicit solutions of Fisher's equation for a special wave speed, Bulletin of Mathematical Biology 41 (1979) 835-840.
[35] D.S. Jone, B.D. Sleeman, Differential Equations and Mathematical Biology, Chapman & Hall/CRC, New York, 2003.
[36] T. Kawahara, M. Tanaka, Interactions of traveling fronts: an exact solution of a nonlinear diffusion equation, Physics Letters A 97 (8) (1983) 311-314.